scientific reports

Check for updates

OPEN

Stanniocalcin-1 promotes temozolomide resistance of glioblastoma through regulation of MGMT

Chao Duan[1,2,5], Bincan He[2,5], Yiqi Wang[1,2], Wanying Liu[2], Wendai Bao[2], Li Yu[1], Jinxin Xin[1], Hui Gui[1], Junrong Lei[3], Zehao Yang[3], Jun Liu[3], Weiwei Tao[2], Jun Qin[3]✉, Jie Luo[3]✉ & Zhiqiang Dong[1,2,4]✉

Temozolomide (TMZ) resistance is a major challenge in the treatment of glioblastoma (GBM). Tumour reproductive cells (TRCs) have been implicated in the development of chemotherapy resistance. By culturing DBTRG cells in three-dimensional soft fibrin gels to enrich GBM TRCs and performing RNA-seq analysis, the expression of stanniocalcin-1 (STC), a gene encoding a secreted glycoprotein, was found to be upregulated in TRCs. Meanwhile, the viability of TMZ-treated TRC cells was significantly higher than that of TMZ-treated 2D cells. Analysis of clinical data from CGGA (Chinese Glioma Genome Atlas) database showed that high expression of STC1 was closely associated with poor prognosis, glioma grade and resistance to TMZ treatment, suggesting that STC1 may be involved in TMZ drug resistance. The expression of STC1 in tissues and cells was examined, as well as the effect of STC1 on GBM cell proliferation and TMZ-induced DNA damage. The results showed that overexpression of STC1 promoted and knockdown of STC1 inhibited TMZ-induced DNA damage. These results were validated in an intracranial tumour model. These data revealed that STC1 exerts regulatory functions on MGMT expression in GBM, and provides a rationale for targeting STC1 to overcome TMZ resistance.

Keywords Glioblastoma, Stanniocalcin-1, Temozolomide, DNA damage, MGMT

Glioblastoma (GBM) is the most common primary brain tumor in adults and is one of the most lethal malignancies because of its aggressive and highly infiltrative nature[1]. The current standard therapy of GBM involves maximum safe surgical resection followed by chemotherapy with Temozolomide (TMZ) and/or radiotherapy, which leads to a mean patient survival of only 15 months[2,3]. TMZ is an alkylating agent and has been considered the first-line chemotherapy agent for postoperative GBM in recent years. Antitumor effect of TMZ depends on its ability to deliver a methyl group to the purine bases of DNA (N7-guanine, N3-guanine, O6-guanine, and N3-adenine), which can induce cell cycle arrest at G_2/M and eventually lead to apoptosis[4]. The therapeutic effect of TMZ is limited, largely due to intrinsic or acquired resistance in GBM[5]. Previous studies have indicated that TMZ resistance is associated with the expression of DNA alkylating proteins and DNA repair enzymes. The primary cytotoxic lesion, O6-methylguanine (O6-MeG), can be removed by methylguanine methyltransferase (MGMT; direct repair) in tumors expressing this protein[6,7] or tolerated in mismatch repair deficient (MMR) tumors[8,9]. Thus, MGMT or MMR deficiency confers TMZ resistance. Other molecular mechanisms, including DNA repair systems[9], aberrant signaling pathways[10], autophagy[11], epigenetic modifications[12], microRNAs[13], and extracellular vesicle production[14], have been identified in recent years. Despite the progressively uncovered mechanisms, TMZ resistance remains a major limitation in GBM treatment. Therefore, unveiling new players in TMZ resistance is required for the development of novel and effective therapeutic approaches to overcome TMZ resistance and improve patient prognosis.

[1]Center for Neurological Disease Research, Taihe Hospital, Hubei University of Medicine, 32 Renmin South Rd, Shiyan 442000, Hubei, China. [2]College of Biomedicine and Health, College of Life Science and Technology, Huazhong Agricultural University, Wuhan 430070, Hubei, China. [3]Department of Neurosurgery, Taihe Hospital, Hubei University of Medicine, 32 Renmin South Rd, Shiyan 442000, Hubei, China. [4]Central Laboratory, Hubei Cancer Hospital, Wuhan 430070, Hubei, China. [5]These authors contributed equally to this work: Chao Duan and Bincan He. ✉email: qingjunxl@163.com; luojie_001@126.com; dongz@mail.hzau.edu.cn

Tumor repopulating cells (TRCs) are cancer stem-like cells (CSC) with high tumorigenic and self-renewing abilities[15]. TRCs exhibit high chemoresistance to conventional chemotherapeutic drug treatment and are therefore key players in cancer relapse after chemotherapy[16–18]. Besides using cell surface markers, including CD44, CD24, and CD133[19], TRCs can also be selected by culturing tumor cells in soft three-dimensional (3D) fibrin gels. When the 3D fibrin gel-selected melanoma TRCs were injected into the tail veins, as few as ten cells could generate distant metastatic tumors in the lungs of wild-type non-syngeneic mice[20]. GBM TRCs are among the major contributors to temozolomide (TMZ) resistance in GBM[21]. Our data also showed that GBM TRCs enriched by 3D fibrin gel culture had higher TMZ resistance. However, the gene expression landscape of these GBM TRCs has not been systemically defined, and the key molecules involved in TMZ resistance remain elusive.

Stanniocalcin-1 (STC1) is a secreted glycoprotein that is expressed in a wide variety of tissues and is involved in many biological processes, such as the regulation of calcium and phosphate balance[22], anti-apoptosis, anti-inflammatory, angiogenesis[23], and glucose metabolism[24]. STC1 has been shown to be highly expressed in tumor tissues and play an important role in tumor progression[25]. High expression of STC1 increases the invasion of cancer cells through the JNK pathway and promotes metastasis[26–29]. *STC1* was reported to be a potential TMZ response-related gene[30], but the role and mechanisms of STC1 in TMZ resistance are unknown.

In this study, we identified STC1 as one of the significantly differentially expressed genes (DEGs) in GBM TRCs. Our analyses on clinical data from CGGA (Chinese Glioma Genome Atlas) database revealed that high STC1 expression was highly associated with poor prognosis, glioma grade, and resistance to TMZ therapy, suggesting the involvement of STC1 in TMZ resistance. GBM cell proliferation and DNA damage were then evaluated both in vivo and in vitro to investigate the effect of knockdown and overexpression of STC1 on TMZ efficacy.

Results

Transcriptome analysis revealed different gene expression landscapes between GBM TRCs and 2D adherent cells

We employed the GBM cell line DBTRG to investigate the gene expression differences between TRCs enriched by 3D fibrin gel culture and 2D conventionally cultured adherent cells. DBTRG cells gradually formed spheres in the fibrin gel, as shown by growth dynamics (Fig. 1A). Compared with the 2D adherent cells, the 3D cultured TRCs expressed higher levels of CD133, SOX2 and Nestin (Fig. S1A), consistent with the stem-like cell properties of TRCs. To explore the molecular mechanisms underlying the phenotype of TRCs, TRCs and adherent cells were harvested separately for RNA-seq analysis after culturing for 5 days. DEGs were filtered under the condition of both p-value < 0.05 and [log2FoldChange (log2FC)] > 1. A total of 1347 DEGs were identified, including 1016 upregulated genes and 331 downregulated genes in TRCs compared to adherent cells (Fig. 1B, Fig. S1B). TRCs and 2D adherent cells have distinct gene expression landscapes, as shown in the heatmap of the top 100 DEGs (Fig. 1C). GO analysis showed that the DEGs were significantly enriched in terms that correlated with cell-microenvironment interactions, such as molecular function (MF) terms of chemorepellent activity, semaphorin receptor binding, and amyloid binding (Fig. 1D, Fig. S1C–D). We further examined the expression of the top upregulated genes using qRT-PCR, which confirmed the increased expression of eight genes, including *FOSB*, *FOS*, *STC1* (Fig. 1E).

STC1 expression is upregulated in GBM tissues and associated with poor prognosis and TMZ resistance in GBM patients.

We analyzed the clinical data from the CGGA database to explore the correlation between the top eight upregulated genes in GBM TRCs and the prognosis of 422 GBM patients. The results showed that, in both primary GBM patients and recurrent GBM patients, high expression levels of *STC1* were associated with poor PFS (Fig. S2A–B). In addition, *STC1* expression was positively correlated with glioma grade in the CGGA RNA-seq database (n = 57 for low-grade glioma, n = 217 for high-grade glioma, $p < 0.001$, Fig. S2C). Next, we examined STC1 expression by immunostaining in grade II and grade IV glioma samples, and the results showed that grade IV gliomas expressed more STC1 than grade II gliomas (Fig. 2A). We further examined the STC1 protein levels in TRCs and 2D adherent cells by western blotting, which showed that GBM TRCs expressed more STC1 protein than 2D adherent cells (Fig. 2B). We subsequently examined the inhibitory effects of TMZ on GBM TRCs and 2D-cultured GBM cells by treating DBTRG spheres and adherent cells with various TMZ concentrations. The results showed that TMZ treatment exhibited lower cytotoxicity to GBM TRCs than to 2D adherent cells at the same concentration (Fig. 2C). Interestingly, our analyses of TMZ-treated samples in the CGGA database revealed that *STC1* expression was significantly increased with TMZ treatment (Fig. S3A). Except for *STC1*, six of the remaining upregulated genes did not show significant correlation with GBM prognosis or TMZ treatment (Figs. S2 and S3), and no data were available on *SPINK1* in the CGGA database. Therefore, we focused on *STC1* in subsequent experiments. We established TMZ-resistant GBM cell lines by treating U87-MG, U251-MG, and a patient-derived cell line (2020260) with progressive TMZ concentration gradients. In accordance with clinical data, TMZ-resistant cells expressed significantly more STC1 than the corresponding controls (Fig. 2D). In summary, our results showed a strong correlation between high expression levels of *STC1* and TMZ resistance in GBM patients, indicating that *STC1* might play an important role in TMZ resistance in GBM.

Overexpression of STC1 promotes TMZ resistance in cultured GBM cells

To further investigate the effect of high STC1 expression on TMZ treatment efficacy, we constructed 2 independent *STC1* over-expressing GBM cell lines, DBTRG-*STC1* OE and U87-MG-*STC1* OE. Overexpression of *STC1* was confirmed by both qRT-PCR and western blot analyses (Fig. 3A–D). Next, we used a colony formation assay to examine the effects of STC1 overexpression on the sensitivity of GBM cells to TMZ treatment.

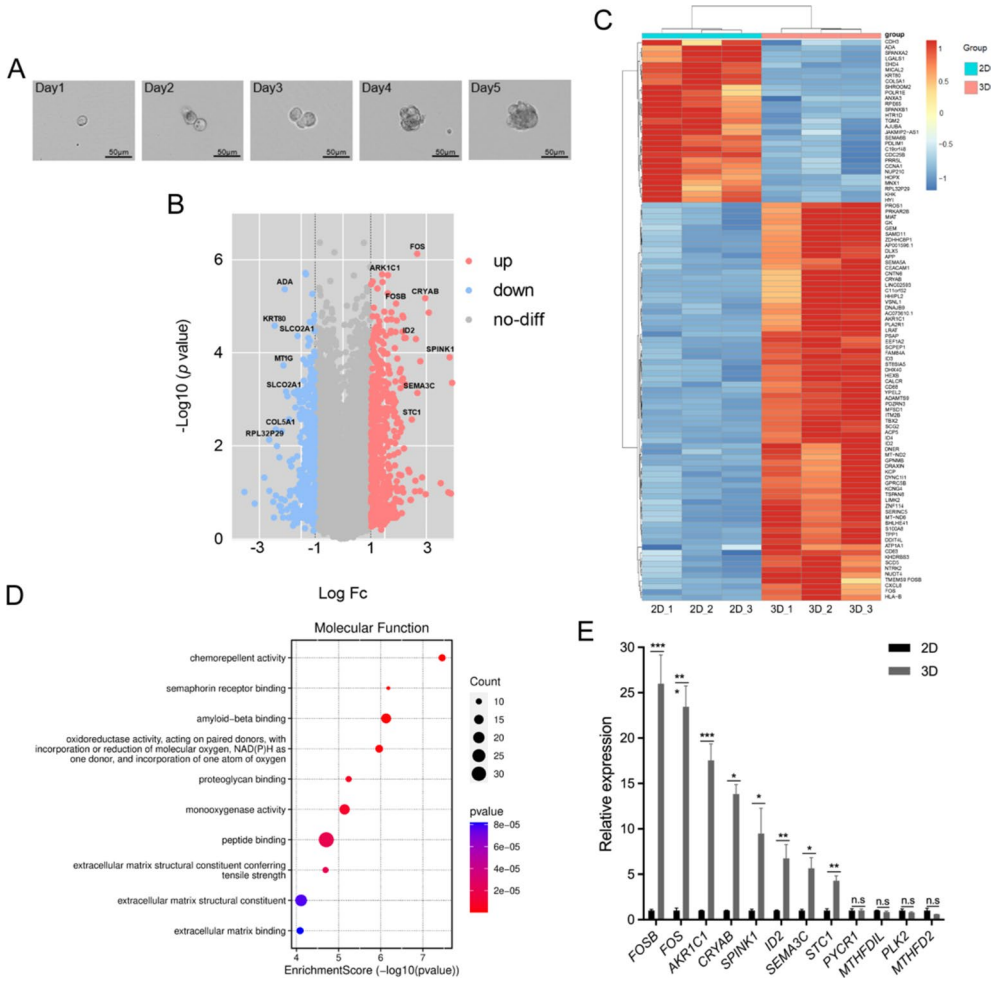

Figure 1. Transcriptome analysis of DEGs between DBTRG TRCs and 2D-cultured adherent cells. (**A**) Images show DBTRG spheres cultured in 3D soft fibrin gel from day1 to day5. (**B**) Volcano map shows the DEGs between DBTRG TRCs and 2D-cultured adherent DBTRG cells disclosed by RNA-seq. (**C**) Heat map shows the top 100 DEGs with the highest *p* value. (**D**) GO_MF enrichment analysis of the DEGs. (**E**) Verification of upregulated genes of interest by qRT-PCR versus 2D. *: $p < 0.05$, **: $p < 0.01$, ***: $p < 0.001$.

The results showed that both DBTRG-*STC1* OE cells (Fig. 3E) and U87-MG-*STC1* OE cells (Fig. 3F) were significantly more resistant to TMZ than the corresponding controls. The resistance-promoting effect of STC1 overexpression was further confirmed by CCK8 analysis, which demonstrated that the TMZ IC50 of in *STC1* OE cells was significantly increased in both GBM cell lines (Fig. 3G, H). As TMZ promotes cell apoptosis by inducing DNA strand breaks during cell replication, we performed Annexin V-PI staining to examine TMZ-induced apoptosis of STC1-overexpressing and control GBM cells. The results revealed that the overexpression of STC1 significantly alleviated TMZ-induced apoptosis in DBTRG cells (Fig. 3I). Taken together, our results suggest that overexpression of STC1 robustly promotes resistance to TMZ in cultured GBM cells.

Overexpression of STC1 facilitates the resistance to TMZ in intracranial GBM xenograft in mice

To investigate the effect of STC1 overexpression on the efficacy of TMZ treatment in vivo, we constructed luciferase-expressing cell lines using DBTRG-*STC1* OE and DBTRG-Ctrl cells and established xenografted tumors by intracranial injection of DBTRG-Luc-*STC1* OE and DBTRG-Luc-Ctrl cells into the right brain of nude mice. The bioluminescence of the xenograft tumors was then measured using a bioluminescence in vivo imaging system every week. When the bioluminescence reached 10^7/s/mm^2/sr, DBTRG-Luc-*STC1* OE and DBTRG-Luc-Ctrl tumor-bearing mice were randomly divided into two groups to receive treatment with either vehicle or 60 mg/kg TMZ for 2 weeks. Tumor growth, as evidenced by the bioluminescence intensity, and survival of tumor-bearing mice were inspected periodically. The results indicated that STC1 overexpression decreased the inhibitory effect of TMZ, leading to increased tumor growth (Fig. 4A, B) and decreased survival rate (Fig. 4C) in the *STC1* OE_TMZ group compared with the Ctrl_TMZ group. Although there was no statistically significant difference in tumor proliferation or survival curves between STC-OE_TMZ and Ctrl_TMZ, the data trends suggest that high STC1 expression may result in shorter survival times for tumor-bearing mice and decrease the therapeutic efficacy of TMZ. The results were further confirmed by hematoxylin and eosin (H&E) staining

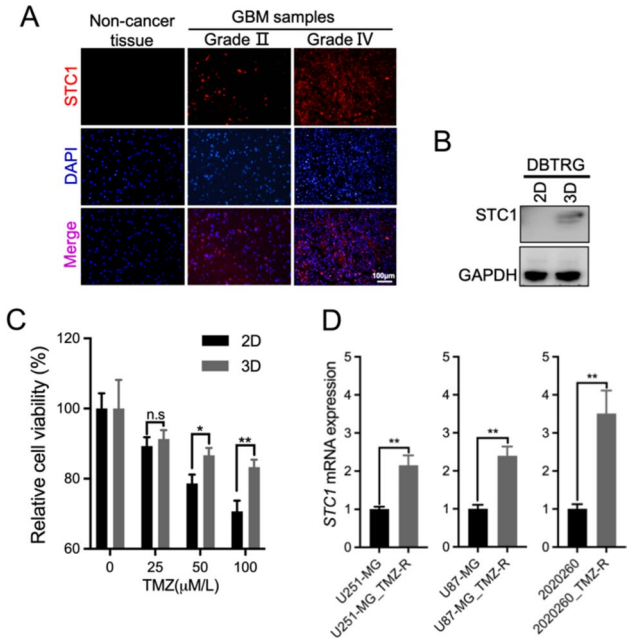

Figure 2. High STC1 expression is associated with poor prognosis and high TMZ resistance in GBM patients. (**A**) Representative images of IF staining shows the expression of STC1 in GBM tissues (scale bar, 100 μm). (**B**) Western blot results show that the expression of STC1 protein is higher in DBTRG TRCs than that in 2D adherent cells. (**C**) Response of DBTRG TRCs and 2D-cultured adherent cells to different dose of TMZ treatment. (**D**) The expression of *STC1* mRNA is higher in TMZ-resistant cells compared with corresponding controls determined by qRT-PCR. **: $p < 0.01$.

of xenografted tumors (Fig. 4D). There was no significant difference in the body weights of the mice among all groups (Fig. 4E). Furthermore, TMZ-induced DNA damage and apoptosis induced by the expression of γ-H2AX and Caspase-3, were significantly inhibited by STC1 overexpression (Fig. 4F, G). Therefore, consistent with the in vitro experiments, the results from tumor-bearing mice indicated that STC1 overexpression enhanced TMZ resistance in grafted GBM tumors.

Knockdown of STC1 promotes TMZ-induced inhibition and apoptosis of cultured GBM cells

To determine whether high STC1 expression is essential for TMZ resistance, we investigated the effect of *STC1* knockdown on TMZ efficacy. Three short hairpin RNAs (shRNAs) targeting *STC1* were designed and tested. Next, we cloned shRNAs into a lentivirus vector containing a doxycycline (Dox)-inducible promoter. DBTRG and U87-MG cells were then infected and doxycycline was added to the culture medium to control the expression of *STC1* shRNAs. We performed qRT-PCR and western blotting to determine the knockdown efficiency. The results showed that all three shRNAs significantly decreased the mRNA and protein expression levels of *STC1* in both the cell lines (Fig. 5A–D). To balance knockdown efficiency and cell viability, we chose shRNA-1 for DBTRG and shRNA-3 for U87-MG cells to establish stable cell lines for subsequent experiments. We examined the viability of *STC1* shRNA-bearing GBM cells treated with or without doxycycline and TMZ treatment at different concentrations. As shown in Fig. 5E, F, *STC1* knockdown enhanced the sensitivity of GBM cells to TMZ in both U87-MG and DBTRG cells, as the IC50 of TMZ in *STC1*-knockdown cells was significantly reduced compared with that in control cells. Likewise, colony formation of *STC1*-knockdown cells was more suppressed by TMZ treatment compared with control cells (Fig. 5G, H). Furthermore, Annexin V/PI staining showed that the apoptosis rate of *STC1*-knockdown cells was significantly higher than that of control cells after 72 h of TMZ treatment (Fig. 5I), suggesting that *STC1* knockdown increased TMZ-induced apoptosis in GBM cells.

Knockdown of STC1 increases TMZ efficacy in intracranial GBM xenograft in mice

To explore the effect of *STC1* knockdown on TMZ efficacy in vivo, we established grafted GBM tumors by intracranial injection of luciferase-expressing DBTRG-Dox-sh*STC1*-1 cells into the right brain of nude mice. The bioluminescence of the tumor xenograft tumors was then measured every week. When the bioluminescence reached 10^7/s/mm^2/sr, tumor-bearing mice with or without doxycycline feeding were randomly divided into two groups to receive either vehicle or 60 mg/kg TMZ for 2 weeks (Fig. 6A). The results showed that STC1 knockdown or TMZ treatment alone inhibited tumor growth by ~ 40–50%, whereas the combination of STC1 knockdown and TMZ treatment inhibited tumor growth by ~ 80–90% (Fig. 6B). Consistent with the tumor growth data, the mouse survival data demonstrated that the 50% survival rate increased from 42.5 days (shSTC1_Dox (–) _Vehicle group) to 56 days (shSTC1_Dox (+) _TMZ group, $p < 0.05$; Fig. 6C). Although there was no statistically significant difference in tumor proliferation and survival curves between shSTC1_Dox(+) _TMZ group and

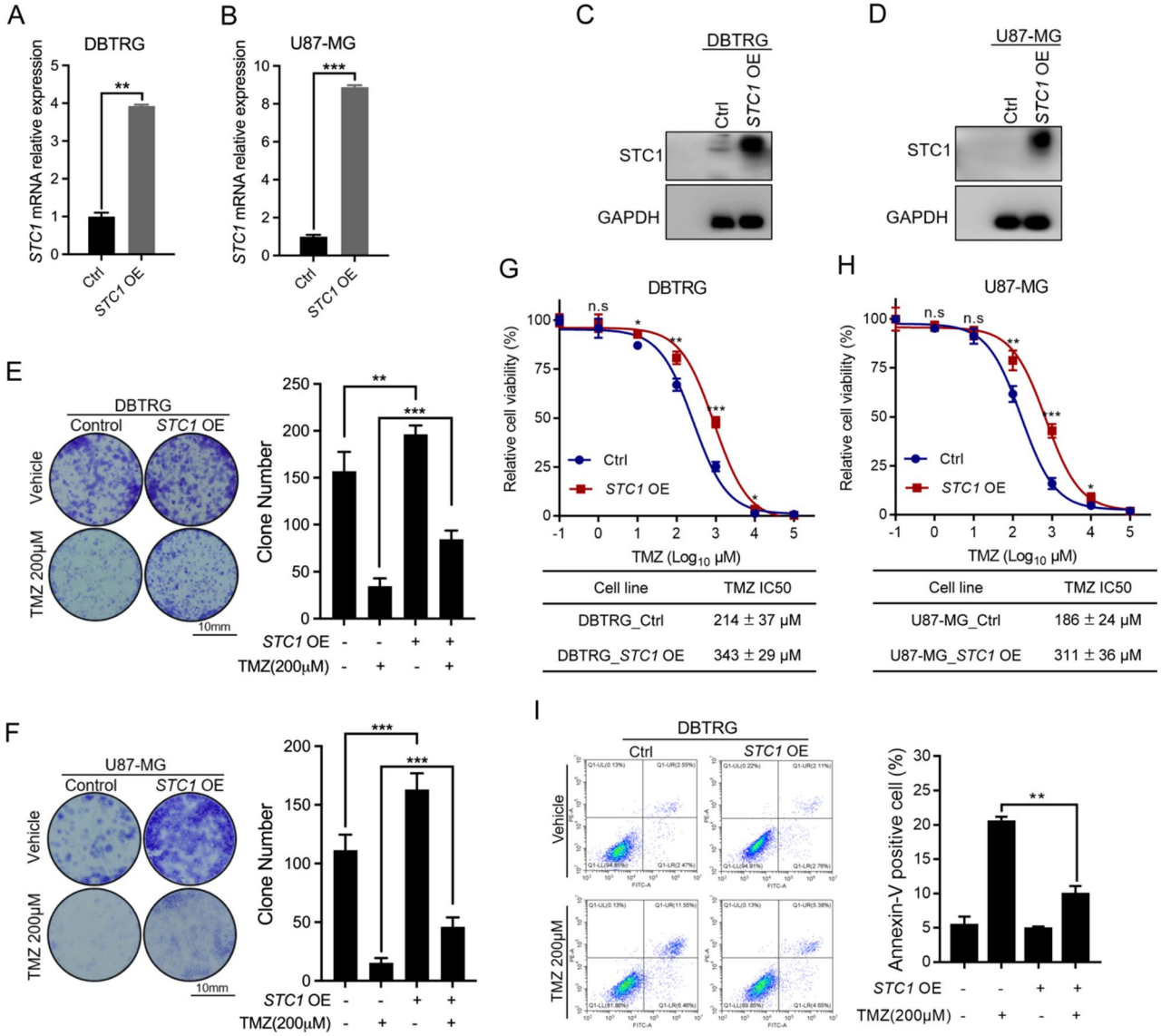

Figure 3. STC1 overexpression increased TMZ resistance in cultured GBM cells. (**A**, **B**) Validation of STC1 overexpression in DBTRG and U87-MG cells by qRT-PCR and (**C**, **D**) western blot. (**E**–**F**) Representative images (left panels) and quantification (right panels) of the colony formation assays on STC1-overexpressing DBTRG (**E**) and U87-MG (**F**) cells treated with 200 μM TMZ (scale bar, 10 mm). (**G**–**H**) Cell viability and IC50 values of TMZ treatment for 72 h in DBTRG (**G**) and U87-MG (**H**) cells. (**I**) Images (left panels) and quantification (right panels) of flow cytometry on TMZ-induced apoptosis in STC1-overexpressing DBTRG cells. *: $p < 0.05$, **: $p < 0.01$, ***: $p < 0.001$.

shSTC1_Dox(−) _TMZ group, the data shapes suggest the STC1 knockdown extended the survival period of tumor-bearing mice and improved the therapeutic efficacy of TMZ. HE staining of xenografted tumors further confirmed that STC1 knockdown enhanced TMZ efficacy in vivo (Fig. 6D). There was no significant change in the body weight of the mice among all the groups (Fig. 6E). Furthermore, TMZ-induced DNA damage and apoptosis, induced by the expression of γ-H2AX and Caspase-3, were significantly increased by STC1 knockdown (Fig. 6F, G). In summary, both our in vitro and in vivo results indicate that STC1 knockdown promotes the inhibition efficacy of TMZ against GBM.

STC1 modulate the efficacy of TMZ by regulating the expression of MGMT

TMZ inhibits tumor progression by causing DNA alkylation damage to induce cell cycle arrest at G_2/M, which eventually leads to apoptosis[31]. To explore the underlying mechanisms by which STC1 regulates TMZ efficacy, we first examined the changes in DNA damage and expression of DNA repair-related proteins in *STC1*-OE/knockdown GBM cells after TMZ treatment. As shown in Fig. 7A and C, overexpression of STC1 significantly reduced TMZ-induced DNA damage compared to that in the control group in the comet assay and γ-H2AX foci assay. In addition, the expression of γ-H2AX, a DNA double-strand break marker, was significantly downregulated, whereas the expression of MGMT was upregulated in STC1-OE cells. Interestingly, in both

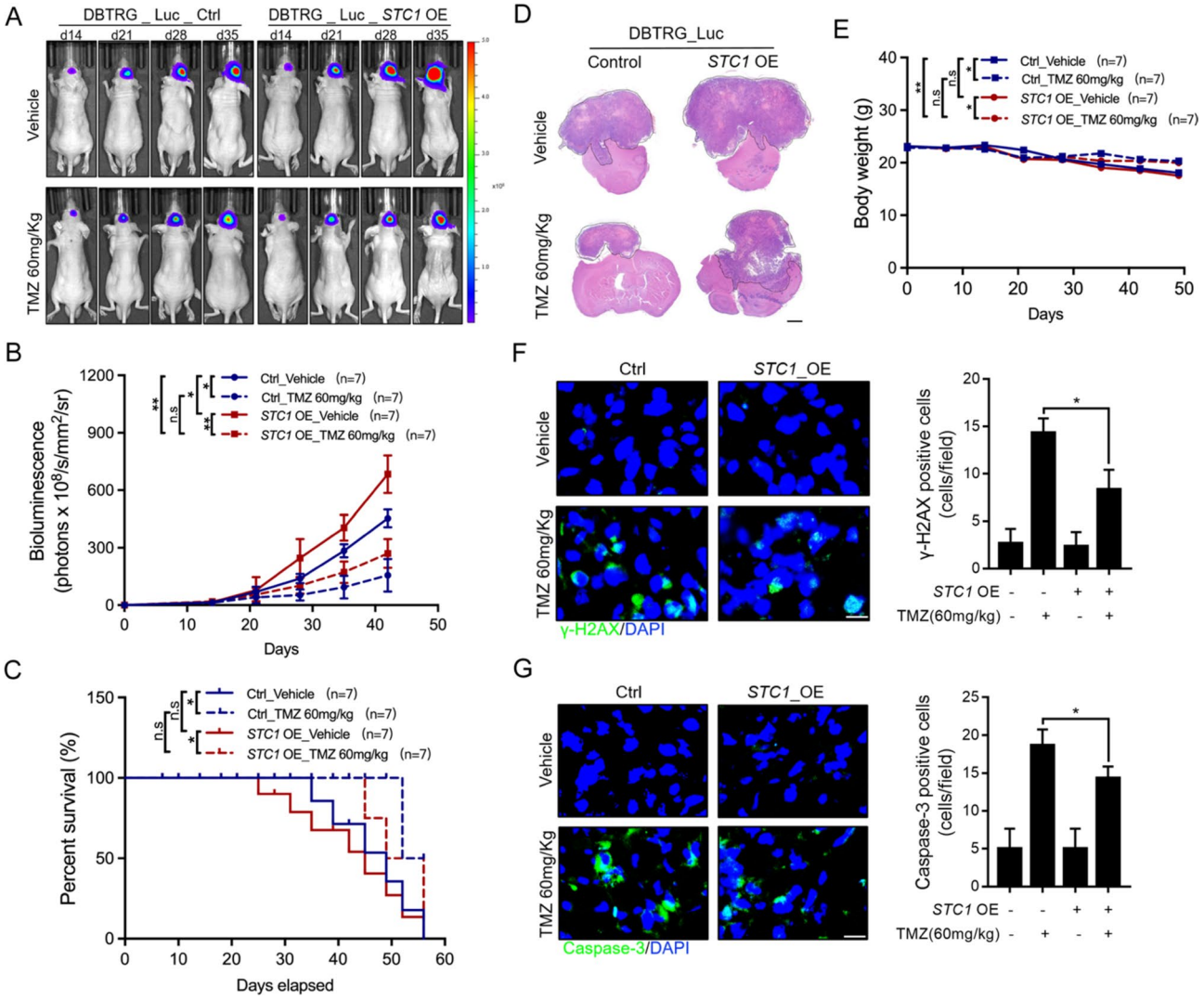

Figure 4. STC1 overexpression increased TMZ resistance in GBM xenografts in mice. (**A**) Images show the retention of bioluminescence of GBM xenografts in mice of different groups treated with TMZ or vehicle. The scale of the luminance bar (right side of images) was kept equal among all images. (**B**) Bioluminescence of GBM xenografts in mice of different groups treated with TMZ or vehicle on day 14, 21, 28, 35, 42 after intracranial cell injection. (**C**) Survival curves of mice in different groups. (**D**) Representative images of H&E-stained sections of the brain tissue with inoculated GBM from different groups (scale bar, 1 mm). (**E**) Body weights of mice from different groups. (**F**) Representative images of immunofluorescence staining (left panels) and quantification (right panels) of double-stranded DNA breaks marker γ-H2AX from different groups (scale bar, 100 μm). (**G**) Representative images of immunofluorescence staining (left panels) and quantification (right panels) of apoptosis marker Caspase3 from different groups (scale bar, 100 μm). *: $p < 0.05$.

TMZ groups and non-TMZ groups, MGMT expression was significantly upregulated by STC1 overexpression, suggesting that STC1 promoted basal and TMZ-induced MGMT expression (Fig. 7B). In contrast, when *STC1* was knocked down in TMZ-treated GBM cells, DNA damage was significantly increased (Fig. 7D and F), while MGMT expression was reduced (Fig. 7E). We further examined MGMT expression in GBM xenografts in mice using immunohistochemical staining. The results showed that in the GBM xenografts of mice treated with TMZ, MGMT expression was increased when STC1 was overexpressed (Fig. 7G) and decreased when *STC1* was knocked down (Fig. 7I). Previous studies have established that activation of the transcription factor STAT3 could regulate MGMT expression[32,33]. Therefore, we explored whether STC1 regulates MGMT expression via the STAT3 pathway. We examined the expression of phosphorylated STAT3 Y705 ((p-STAT3 (Y705)), which is generally believed to be essential for the transcriptional activity of STAT3, together with total STAT3 and MGMT in both STC1-OE and *STC1*-knockdown DBTRG cells treated with vehicle or 200 μM TMZ for 72 h. Consistent with the above data, the expression of p-STAT3 and MGMT was enhanced by TMZ treatment in DBTRG cells. Furthermore, overexpression of STC1 was enhanced, while knockdown of *STC1* decreased the expression of p-STAT3 and MGMT (Fig. 7H, J), indicating that STC1 probably regulates MGMT expression by modulating the expression of p-STAT3 in GBM cells.

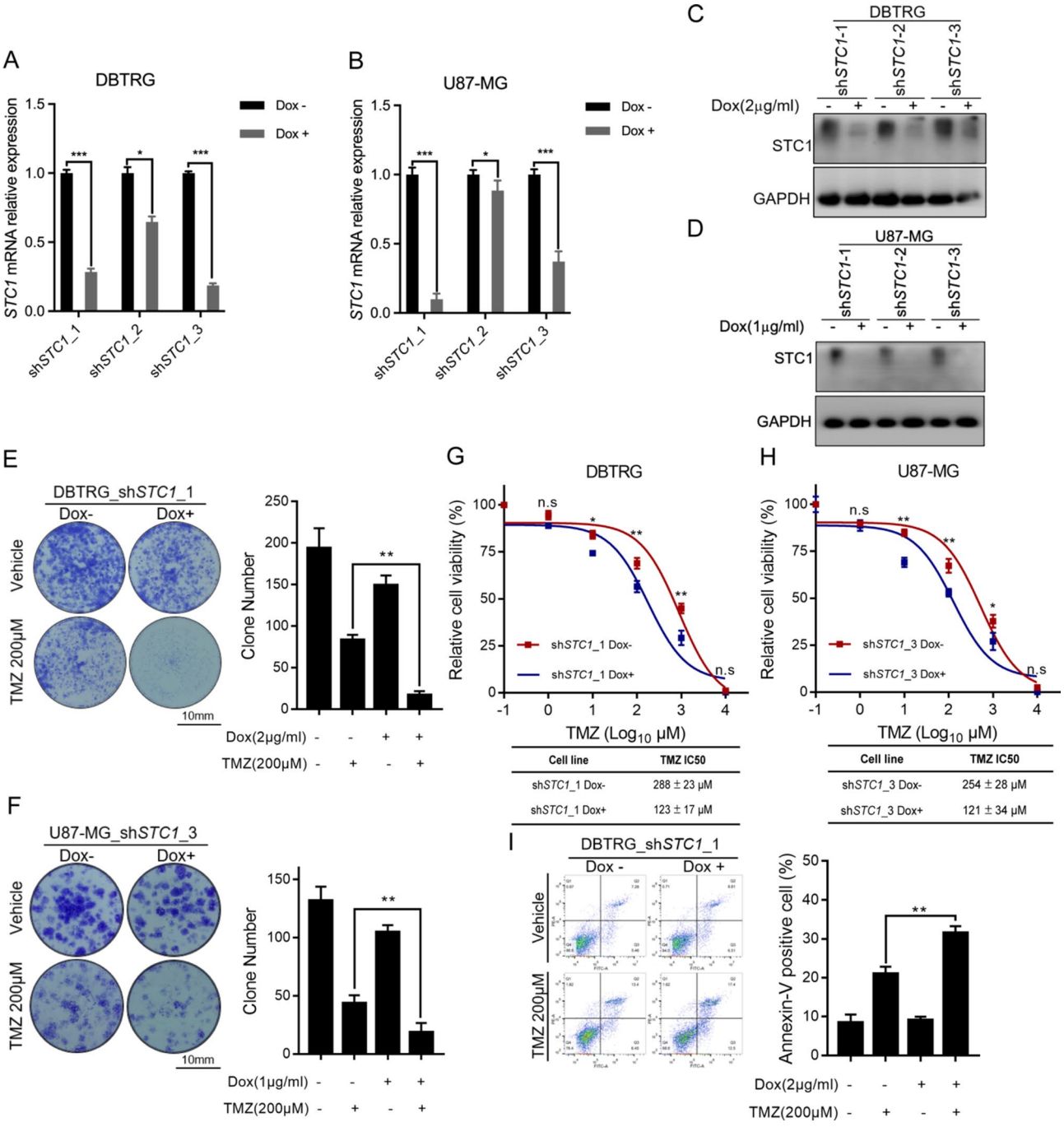

Figure 5. STC1 knockdown enhanced the inhibition and apoptosis of cultured GBM cells induced by TMZ treatment. (**A**–**B**) Validation of STC1 knockdown in GBM cell lines by qRT-PCR and (**C**–**D**) Western blot. (**E**–**F**) Representative images (left panels) and quantification (right panels) of the colony formation assays on STC1-knockdown DBTRG (**E**) and U87-MG (**F**) cells treated with 200 μM TMZ (scale bar, 10 mm). (**G**–**H**) Cell viability and IC50 values of TMZ treatment for 72 h in DBTRG (**G**) and U87-MG (**H**) cells. (**I**) Images (left panels) and quantification (right panels) of flow cytometry on TMZ-induced apoptosis in DBTRG STC1-knockdown cells. *: $p < 0.05$, **: $p < 0.01$, ***: $p < 0.001$.

Discussion

TRCs, also called CSC-like cells, have been proved to be responsible for the chemotherapy resistance, recurrence and malignancy progression of cancers[34,35]. There are various methods to enrich CSC-like cells, such as the use of conventional cell surface markers, such as CD133 and CD44. Previous studies have developed mechanical methods to select and grow TRCs in 3D soft fibrin gels[20]. We adopted this method and reliably enriched GBM TRCs, as evidenced by the expression of CSC surface markers CD133 and SOX2, as well as increased resistance to TMZ in selected TRCs. We systemically dissected and compared the transcriptomic landscapes of DBTRG TRCs

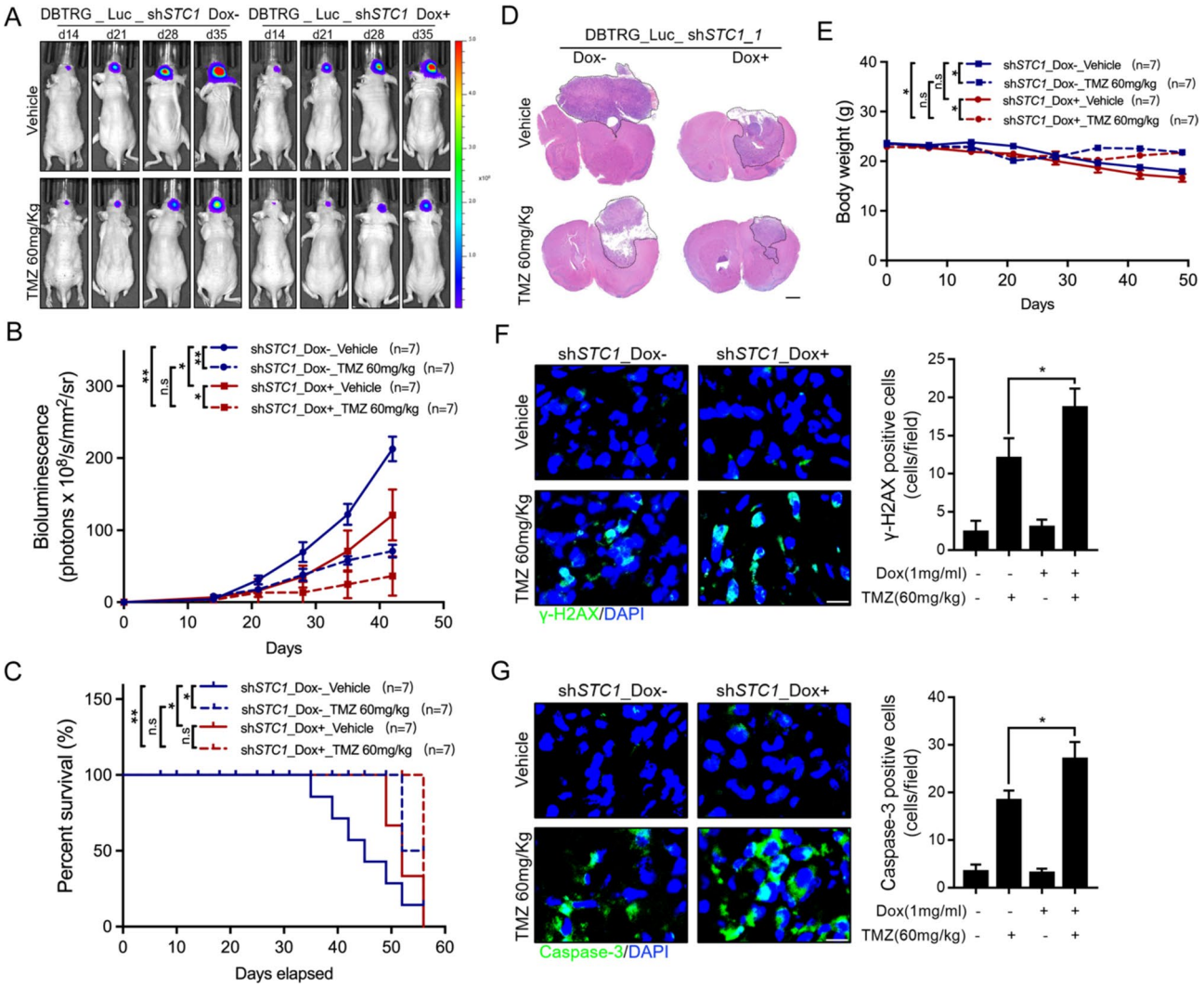

Figure 6. STC1 knockdown increase TMZ efficacy in GBM xenografts in mice. (**A**) Images show the retention of bioluminescence of GBM xenografts in mice of different groups treated with TMZ or vehicle. The scale of the luminance bar (right side of images) was kept equal among all images. (**B**) Bioluminescence of GBM xenografts in mice of different groups treated with TMZ or vehicle on day 14, 21, 28, 35, 42 after intracranial cell injection. (**C**) Survival curves of mice in different groups. (**D**) Representative images of H&E-stained sections of the brain tissue with inoculated GBM from different groups (scale bar, 1 mm). (**E**) Body weights of mice from different groups. (**F**) Representative images of immunofluorescence staining (left panels) and quantification (right panels) of double-stranded DNA breaks marker γ-H2AX from different groups (scale bar, 100 μm). (**G**) Representative images of immunofluorescence staining (left panels) and quantification (right panels) of apoptosis marker Caspase3 from different groups (scale bar, 100 μm). *: $p < 0.05$, **: $p < 0.01$.

and conventional 2D-cultured cells, providing a useful resource for the GBM research community. Furthermore, TRCs enriched by 3D soft fibrin gels can be useful tools for drug screening to develop novel strategies for GBM treatment.

Thus, we revealed the crucial role of STC1 in TMZ resistance. STC1 is a hormone-like protein that exists in the extracellular matrix (ECM) and is involved in many biological and pathological processes[22]. Previous studies have shown that STC1 can be used as a diagnostic and prognostic molecule for multiple cancers[36–38] and plays an important role in chemotherapy resistance[39]. STC1 is a phagocytosis checkpoint that drives tumor immune resistance[40]. STC1 activation promotes sphere formation and tumorigenic ability of cancer stem-like cells[41,42]. STC1 has also been shown to be crucial for cisplatin chemoresistance in ovarian cancer cells by regulating the FOXC2/ITGB6 signaling axis[43]. Consistent with the reported role of STC1 in various cancers, our study showed that STC1 expression is upregulated and is associated with poor prognosis and TMZ resistance in patients with GBM. We further demonstrated that STC1 promoted TMZ resistance in GBM cells through the STAT3-mediated upregulation of MGMT (Fig. S4). Nonetheless, the receptor of STC1 and its interaction partners are largely unknown, the clarification of which would help further elucidate the mechanism and identify new regulators.

Our results indicated that in addition to promoting TMZ resistance, STC1 could also regulate GBM cell proliferation, as STC1 overexpression increased while knockdown decreased GBM cell proliferation, which was

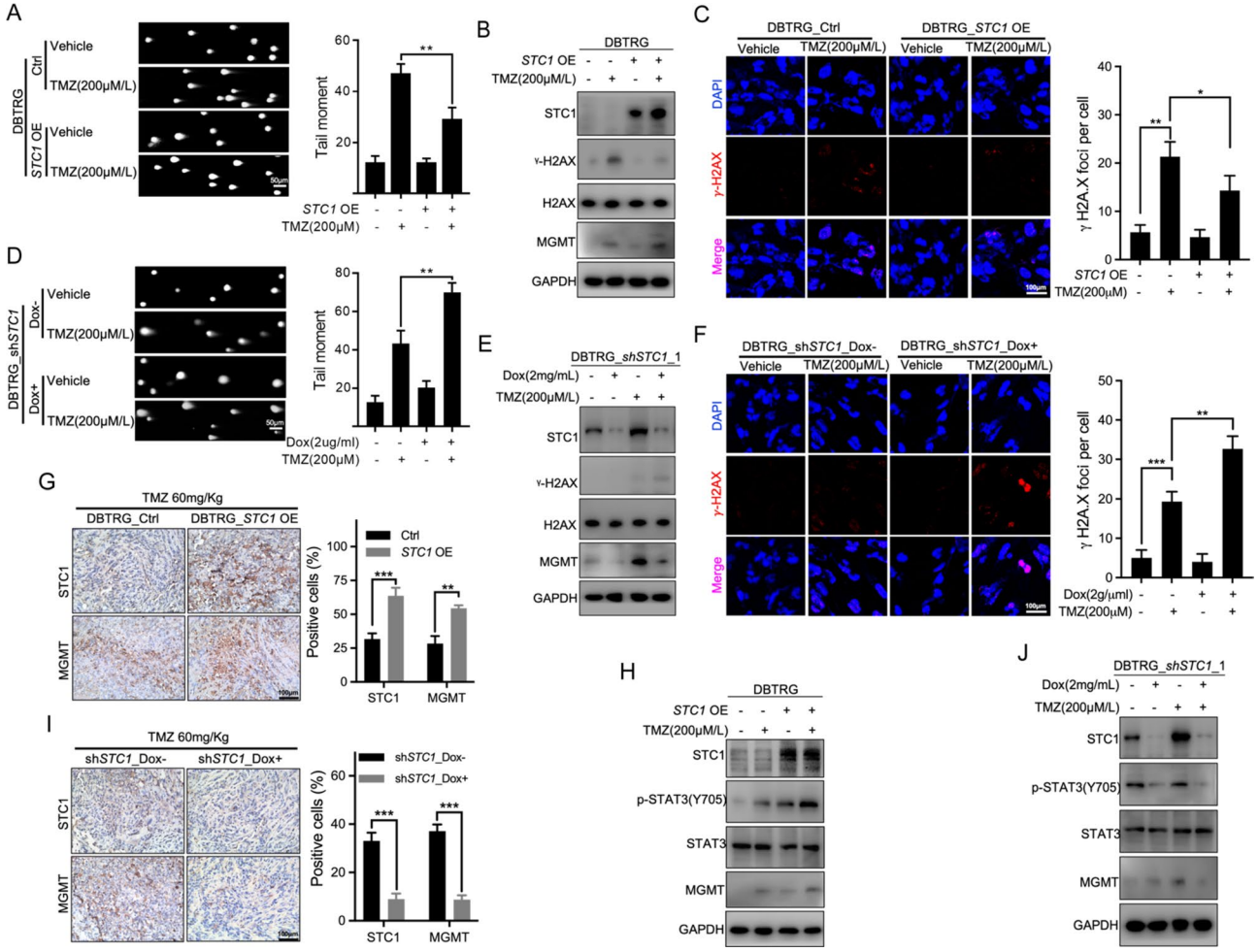

Figure 7. STC1 enhanced TMZ-induced DNA damage through STAT3-mediated inhibition of MGMT expression. (**A**, **D**) Representative images (left panel) and quantification (right panel) of comet assay on STC1-overexpressing (**A**) or *STC1*-knockdown (**D**) DBTRG cells treated with vehicle or 200 μM TMZ for 72 h. (**B**, **E**) Western blot results shows the protein expression of double-stranded DNA break marker γ-H2AX, the total H2AX and MGMT in STC1-overexpressing (**B**) or *STC1*-knockdown (**D**) DBTRG cells treated with vehicle or 200 μM TMZ for 72 h. (**C**, **F**) Representative images (left panel) and quantification (right panel) of γ-H2AX foci staining on STC1-overexpressing (**C**) or *STC1*-knockdown (**F**) DBTRG cells treated with vehicle or 200 μM TMZ for 72 h (scale bar, 100 μm). (**G**, **I**) Representative images of immunohistochemistry staining (left panels) and quantification (right panels) of STC1 and MGMT on tumor tissues of mice with intracranial injection of STC1-overexpressing (**G**) or *STC1*-knockdown (**I**) DBTRG cells and treated with vehicle or TMZ (scale bar, 100 μm). (**H**, **J**) Western blot results show the protein levels of phosphorylated STAT3 (p-STAT3(Y705)), STAT3 and MGMT in STC1-overexpressing (**H**) or *STC1*-knockdown (**J**) DBTRG cells treated with vehicle or 200 μM TMZ for 72 h. **: $p < 0.01$, ***: $p < 0.001$.

further confirmed by the fact that STC1-overexpressing DBTRG cells formed more spheres in soft fibrin gel when seeded in the same amount as the control cells (Fig. S1E). Therefore, it is likely that STC1 contributes to the malignant progression of GBM through multiple mechanisms. In this study, we found that STC1 constitutive knockout severely inhibited glioma cell growth, consistent with previous studies showing that STC1 knockout causes cell cycle arrest and growth inhibition[44,45]. In contrast, the altered TMZ resistance caused by manipulating STC1 expression could be partially and indirectly caused by its effects on cell proliferation. However, the direct effects of STC1 on TMZ resistance are confident, as TMZ-induced DNA damage and apoptosis decreased in STC1-overespressing GBM cells and increased in STC1-knockdown cells. Phosphorylation of STAT3 Tyr705 is required for nuclear translocation of STAT3 transcriptional activity, as shown in previous studies[32,46]. Thus, increased STAT3 Tyr705 phosphorylation leads to more nuclear translocation to promote MGMT expression. We propose that both transcriptional and post-transcriptional processes may be involved in the regulation of MGMT expression by STAT3. Actually, we have confirmed the fact that blocking STAT3 phosphorylation reverses MGMT expression and TMZ resistance in our previously published study[47]. This study suggests that STC1 upregulates MGMT expression by activating STAT3 pathway. As the STAT3 pathway has wide effects on cancer cell behavior [48–50] and has been shown to regulate TRC dormancy[51], activation of the STAT3 pathway could also be one of the underlying mechanisms by which STC1 promotes GBM cell proliferation and TMZ resistance. In

summary, our study identified STC1 as an important regulator of TMZ resistance in GBM and could potentially be used as a predictive factor for the efficacy of TMZ treatment. Furthermore, STC1, as well as its receptor and downstream molecules, which require further exploration, can be targets to improve the therapeutic efficacy of TMZ in GBM patients.

In conclusion, we revealed that STC1 expression was increased in tumor repopulating cells and contributed to glioblastoma cells resistant to TMZ. In vitro and in vivo experiments disclosed that high expression of STC1 confer resistance to TMZ, while knockdown of STC1 improves the efficacy of TMZ. Our study also shows that STC1 regulates MGMT expression, which affects TMZ efficacy, by modulating STAT3 activation. Therefore, STC1 could be a prognostic marker for TMZ chemotherapy and a potential molecular target to reverse TMZ resistance.

Materials and methods

Reagent preparation and storage

TMZ was purchased from MedChemExpress (MCE, New Jersey, USA). TMZ was dissolved in DMSO to prepare a stock solution at a concentration of 100 mM, and then TMZ was equipped and wrapped in a brown centrifugal tube for protection against light and stored at − 20 °C. Key materials and information in the article are summarized in Key resources table.

Cell culture

The U251-MG, U87-MG, and DBTRG were purchased from Cell bank of Chinese Academy of Sciences (Shanghai, China), and patient-derived cell line, 2,020,260, acquired from Hubei University of Medicine, Taihe hospital. All cells were cultured in Dulbecco's Modified Eagle's Medium (DMEM, Hyclone) supplemented with 1% Penicillin–Streptomycin and 10% fetal bovine serum (FBS, BI). TMZ resistant cell lines were developed by using the TMZ concentration gradient progressive methods as previous described[52]. Briefly, U251-MG and U87-MG cells at a concentration of 1×10^5/mL were inoculated into TMZ-free culture medium for 24 h until they reached the logarithmic phase. The culture medium was then replaced with that containing a low concentration (10 μM) of TMZ for 72 h, followed by the removal of the culture medium containing drugs and dead cells. The cells were collected and re-inoculated in TMZ-free culture medium to get recovered before the next TMZ treatment. After the cells were adjusted to the present TMZ treatment, the concentration of TMZ was increased in turn until cells survived well and developed resistance to 400 μM TMZ.

In vivo anti-tumor activity

In total, 56 male, 6-week-old nude mice (weight, 20 g) were purchased from the Model Animal Research Center at Nanjing University (Nanjing, China) and housed in accordance with the National Institutes of Health Guide for the Care and Use of Laboratory Animals. To study the role of STC1 in TMZ resistance, the mice were randomly divided into eight groups (n = 7 per group). To establish the GBM models, mice were anesthetized and placed in a stereotact; 3×10^4 Ctrl, *STC1* OE, or sh*STC1* DBTRG-GFP-Luc cells resuspended in 4 μL PBS were injected 2 mm lateral and 1 mm anterior to the bregma, 2 mm below the skull. A total of 10 days later, bioluminescence of the tumor was monitored once a week using an IVIS Spectrum imaging system (PerkinElmer). For TMZ treatment groups, mice injected cells for 14 days were treated with TMZ (at a dose of 60 mg/kg) at the frequency of 5 days on and 2 days off for 2 weeks. Mice were sacrificed when they showed weight loss (> 20%) or neurological symptoms. On day 56, the mice were sacrificed, and their brain tissues were excised, fixed in 4% PFA, and embedded in paraffin for Hematoxylin and Eosin (H&E) and immunohistochemical (IHC) staining. All procedures for the animal experiments were approved by the Animal Care Committee of Hubei University of Medicine (Shiyan, China), and performed in accordance with the institutional guidelines (approval number 2022–022).

3D fibrin gel cell culture of DBTRG cells

Three-dimensional fibrin gel cell culture was performed as previously described[20,53,54]. Salmon fibrinogen and thrombin were purchased from Reagent Proteins (CA, USA). 3D fibrin gels were prepared as described following. Briefly, DBTRG cells were detached and suspended in DMEM cell culture medium (10% FBS, 1% penicillin–streptomycin solution), and cell density was adjusted to 2×10^5 cells/mL. Fibrinogen was diluted to a 2 mg/mL solution containing 50 mM Tris and 150 mM NaCl, pH 7.4. The cell supernatant and fibrinogen solution were mixed in equal volumes and 600 μL of the mixture was added to 24 wells cell plate with 5 μL thrombin (0.1 U/μL). The plate was moved into cell culture incubator (37 °C, 5% CO_2) for 45 min, then add 500 μL DMEM cell culture medium each well. Cells were released by the mechanical force of the tips after 5 days and separated by centrifugation.

Transcriptome analysis

Total RNA was extracted from the cells using TRIzol® reagent, according to the manufacturer's instructions. Quality control of the raw RNA-seq sequences was initially performed according to the Fastp application. Fastp can deal with both trimming and quality control to ensure a high-quality read exercise in the following formal analysis. The application in the reads alignment procedure was Hisat2, whose reference genome was hg38, with the default parameters in our paired reads. The HTSeq package was used to construct a count matrix using the mapping results. DESeq2 was then applied to build a model with the observed counts for differential expression analysis with a threshold log2 FC > ± 1 and p-value < 0.05. The DEGs were enrolled in the enrichment and GSEA analyses using the Cluster Profiler package. Enrichment functions of the corresponding GO process, KEGG[55], and REACTOME pathways were called with filtration cutoff values as both p-value and Q-value (p-adjust) less than 0.01. The plotting built-in function was then invoked for dot plots and heatmap presentation. RNA-seq data were deposited to the GEO database (GSE261684).

Bioinformatic analysis using online databases

Gene expression data and clinical characteristics were acquired from the Chinese Glioma Genome Atlas (CGGA) database (http://www.cgga.org.cn). Data from mRNAseq_325 (containing 325 samples) were used for gene expression analysis of low-grade and high-grade gliomas. Disease-specific overall survival (OS) was calculated from the date of diagnosis until disease-caused death or end of follow-up. Differences in expression features between different groups were determined using Student's t-tests. Kaplan–Meier curves were developed using GraphPad Prism 7 (GraphPad Software Inc., San Diego, CA, USA) to compare the overall survival rates between patients with low and high expression of interest.

Lentivirus production and cell infection

Human *STC1* cDNA was generated and inserted into the lentiviral vector. The pLenti-NC (Ctrl) and pLenti-*STC1*(*STC1* OE) plasmids were transfected into HEK-293 T cells. The supernatant was collected 72 h later. *STC1*-silenced U87-MG/DBTRG cells were established using tet-pLKO.1-puro vector, using a similar strategy. The sequences of the scrambled or human *STC1*-specific shRNAs are listed in Supplementary Table 1.

Quantitative real-time polymerase chain reaction (QRT-PCR)

Cellular RNA was isolated using TRIzol reagent and reverse transcribed to complementary DNA (cDNA) using a cDNA Synthesis Kit (Vazyme). QRT-PCR was performed on an CFX96 Touch Deep Well RT-PCR System using specific primers (Supplementary Table 2). The data were normalized to that of GAPDH.

Cell viability assay

Cell viability was examined using a CCK-8 kit. Briefly, 96-well plates were used for seeding GBM cells at a density of 2×10^3 cells treated with vehicle or TMZ. After 72 h treatment, 10 μL of CCK-8 was added to each well and incubated for an hour at 37 °C. The absorbance at 450 nm was measured and relative cell viability was calculated as: (average A450 of the experimental -average A450 of the blank group) / (average A450 of the control group—average A450 of the blank group) × 100%.

Colony formation assay

To assess the impact of treatment on the clonogenicity of GBM cells, the cells were cultured in 12-well plates for 10–14 days with 200 cells per well. Colonies were then fixed with methanol and stained with crystal violet. The plating efficiency was determined by counting the number of colonies and was calculated as (number of colonies formed/number of cells inoculated) × 100%.

Comet assay

Cells that received vehicle or 200 μM TMZ treatment for 72 h were collected and the comet assay was performed as previously described[47]. In brief, images were acquired using a Leica DMi1 microscope and analyzed using the Comet Score software (CASP, CASP-Lab).

Western blot analysis

Cells were lysed and homogenized in radioimmunoprecipitation assay (RIPA) buffer, and protein concentrations were determined using a BCA Protein Assay Kit (Thermo Fisher, CA, USA). Protein samples were separated using 10% sodium dodecyl sulfate–polyacrylamide gels and transferred to PVDF membranes (Merck Millipore, MA, United States), and the membrane was blocked with 3% bovine serum albumin for 1 h. The blots were incubated with specific primary antibodies 4 °C overnight. The blots were rinsed with TBST (Tris-buffered saline with Tween®20) three times and then incubated with the corresponding horseradish peroxidase-conjugated secondary antibodies for 2 h. Target proteins were visualized using an ECL kit (Merck Millipore, MA, United States), and the density of the immunoreactive bands was analyzed using Imager software (Bio-Rad, California, United States).

Cell apoptosis analysis

The Annexin V-FITC/PE kit (BD Bioscience) was used to examine cell apoptosis. sh*STC1* and *STC1* OE DBTRG cells were treated with 200 μM TMZ for 72 h, collected, stained with 5 μL of Annexin V-FITC for 5 min in the dark, and stained with 10 μL of PE at room temperature. The rate of apoptosis in each sample was analyzed using a flow cytometer (BD FACSCanto II) and calculated using the BD FACS-Diva software.

Immunostaining of Glioblastoma samples and cells

The xenografted tumors were isolated from the brain tissues, embedded in paraffin, sectioned at 6 μm, deparaffinized, and rehydrated. One section of each sample was stained with hematoxylin and eosin (H&E). For immunohistochemistry, antigen retrieved sections were treated with 10 mmol/L citrate buffer (pH 6.0) for 20 min at 95 °C in a laboratory microwave oven, and subsequently washed with PBS. After quenching endogenous peroxidase activity and blocking with normal goat serum, sections were stained using the Bond RX automated immunohistochemistry staining system Bond RX (Leica Biosystems). The primary antibodies used were rabbit anti-STC1 (1:200; ABclonal) and rabbit anti-MGMT (1:400; Abcam). For immunofluorescence, the sections were washed three times with PBS for 10 min each, and then permeabilized in PBS + 0.5% Triton X-100 for 10 min, followed by triple-wash in PBS for 10 min each. The sections were then incubated in blocking solution at room temperature for 1 h. After blocking, the sections were incubated with γ-H2AX (1:300, Abcam) and Caspase-3 (1:200, Abcam) primary antibodies overnight at 4 °C. The sections were washed three times with PBS for 10 min each. Then, 1:500 diluted secondary antibodies against rabbit or mouse were added to the sections and incubated

for 2 h at room temperature. The sections were washed three times with PBS for 10 min each and then incubated with Hoechst solution for 10 min at room temperature. Finally, the stained sections were sealed and imaged.

Statistical analysis

Experiments were performed in triplicate, and GraphPad Prism 7 was used for statistical analyses. Data are presented as mean ± standard deviation (SD). Data between two groups were analyzed using the student's t-test (two-tailed distribution). Data between the three groups were analyzed using one-way ANOVA, followed by Dunnett's multiple comparison test. Statistical significance is described as follows: * $p < 0.05$, ** $p < 0.01$, and *** $p < 0.001$.

Ethical approval and consent to participate

This study was approved by the Medical Ethics Committee of Shiyan Taihe Hospital (reference NO.2023KS09). The animal study protocol was approved by the Institutional Animal Care and Use Committee of Hubei University of Medicine (reference NO.2022022), and this study was reported in accordance with ARRIVE guiledines.

Data availability

Data have been deposited GEO database.The datasets generated and/or analysed during the current study are available in the GEO repository, [www.ncbi.nlm.nih.gov/geo/]. Accession Number: [GSE261684].

Received: 9 January 2024; Accepted: 29 July 2024
Published online: 30 August 2024

References

1. Ostrom, Q. T., Cote, D. J., Ascha, M., Kruchko, C. & Barnholtz-Sloan, J. S. Adult Glioma incidence and survival by race or ethnicity in the United States from 2000 to 2014. *JAMA Oncol.* **4**(9), 1254–1262 (2018).
2. Perry, J. R. *et al.* Short-course radiation plus temozolomide in elderly patients with glioblastoma. *N. Engl. J. Med.* **376**(11), 1027–1037 (2017).
3. Le Rhun, E. *et al.* Molecular targeted therapy of glioblastoma. *Cancer Treat. Rev.* **80**, 101896 (2019).
4. Tomar, M. S., Kumar, A., Srivastava, C. & Shrivastava, A. Elucidating the mechanisms of temozolomide resistance in gliomas and the strategies to overcome the resistance. *Biochim. Biophys. Acta* **1876**(2), 188616 (2021).
5. Lee, S. Y. Temozolomide resistance in glioblastoma multiforme. *Genes Dis.* **3**(3), 198–210 (2016).
6. Wu, S. *et al.* PARP-mediated PARylation of MGMT is critical to promote repair of temozolomide-induced O6-methylguanine DNA damage in glioblastoma. *Neuro-oncology* **23**(6), 920–931 (2021).
7. Kitange, G. J. *et al.* Induction of MGMT expression is associated with temozolomide resistance in glioblastoma xenografts. *Neuro-oncology* **11**(3), 281–291 (2009).
8. Li, G. M. Mechanisms and functions of DNA mismatch repair. *Cell Res.* **18**(1), 85–98 (2008).
9. Lin, K. *et al.* Mechanism-based design of agents that selectively target drug-resistant glioma. *Science (New York, NY)* **377**(6605), 502–511 (2022).
10. Li, J. *et al.* CircTTLL13 Promotes TMZ Resistance in Glioma via Modulating OLR1-Mediated Activation of the Wnt/β-Catenin Pathway. *Mol. Cell Biol.* **43**(7), 354–369 (2023).
11. Lu, H. *et al.* TOPK inhibits autophagy by phosphorylating ULK1 and promotes glioma resistance to TMZ. *Cell Death Dis.* **10**(8), 583 (2019).
12. Yu, T. *et al.* EZH2 interacts with HP1BP3 to epigenetically activate WNT7B that promotes temozolomide resistance in glioblastoma. *Oncogene* **42**(6), 461–470 (2023).
13. Huang, T. *et al.* MIR93 (microRNA -93) regulates tumorigenicity and therapy response of glioblastoma by targeting autophagy. *Autophagy* **15**(6), 1100–1111 (2019).
14. Yin, J. *et al.* Extracellular vesicles derived from hypoxic glioma stem-like cells confer temozolomide resistance on glioblastoma by delivering miR-30b-3p. *Theranostics* **11**(4), 1763–1779 (2021).
15. Tan, Y. *et al.* Matrix softness regulates plasticity of tumour-repopulating cells via H3K9 demethylation and Sox2 expression. *Nat. Commun.* **5**, 4619 (2014).
16. Beier, D., Schulz, J. B. & Beier, C. P. Chemoresistance of glioblastoma cancer stem cells–much more complex than expected. *Mol. Cancer* **10**, 128 (2011).
17. Dean, M., Fojo, T. & Bates, S. Tumour stem cells and drug resistance. *Nat. Rev. Cancer* **5**(4), 275–284 (2005).
18. Shibue, T. & Weinberg, R. A. EMT, CSCs, and drug resistance: The mechanistic link and clinical implications. *Nat. Rev. Clin. Oncol.* **14**(10), 611–629 (2017).
19. Wu, H. J. & Chu, P. Y. Role of cancer stem cells in cholangiocarcinoma and therapeutic implications. *Int. J. Mol. Sci.* **20**(17), 4154 (2019).
20. Liu, J. *et al.* Soft fibrin gels promote selection and growth of tumorigenic cells. *Nat. Mater.* **11**(8), 734–741 (2012).
21. Singh, N., Miner, A., Hennis, L. & Mittal, S. Mechanisms of temozolomide resistance in glioblastoma—a comprehensive review. *Cancer Drug Resist. (Alhambra, Calif)* **4**(1), 17–43 (2021).
22. Yeung, B. H., Law, A. Y. & Wong, C. K. Evolution and roles of stanniocalcin. *Mol. Cell. Endocrinol.* **349**(2), 272–280 (2012).
23. Su, J. *et al.* Stanniocalcin-1, a new biomarker of glioma progression, is associated with prognosis of patients. *Tumour Biol.* **36**(8), 6333–6339 (2015).
24. Zhao, F. *et al.* Expression, function and clinical application of stanniocalcin-1 in cancer. *J. Cell. Mol. Med.* **24**(14), 7686–7696 (2020).
25. Tamura, S. *et al.* Clinical significance of STC1 gene expression in patients with colorectal cancer. *Anticancer Res.* **31**(1), 325–329 (2011).
26. Chan, K. K. *et al.* Secretory Stanniocalcin 1 promotes metastasis of hepatocellular carcinoma through activation of JNK signaling pathway. *Cancer Lett.* **403**, 330–338 (2017).
27. Han, J., Jeon, M., Shin, I. & Kim, S. Elevated STC-1 augments the invasiveness of triple-negative breast cancer cells through activation of the JNK/c-Jun signaling pathway. *Oncol. Rep.* **36**(3), 1764–1771 (2016).
28. Avalle, L. *et al.* STAT3 induces breast cancer growth via ANGPTL4, MMP13 and STC1 secretion by cancer associated fibroblasts. *Oncogene* **41**(10), 1456–1467 (2022).
29. Xiong, Y. & Wang, Q. STC1 regulates glioblastoma migration and invasion via the TGF-β/SMAD4 signaling pathway. *Mol. Med. Rep.* **20**(4), 3055–3064 (2019).
30. Cai, H. Q. *et al.* Identifying predictive gene expression and signature related to temozolomide sensitivity of glioblastomas. *Front. Oncol.* **10**, 669 (2020).

31. Vengoji, R. *et al.* Afatinib and temozolomide combination inhibits tumorigenesis by targeting EGFRvIII-cMet signaling in glioblastoma cells. *J. Exp. Clin. Cancer Res. CR* **38**(1), 266 (2019).
32. Kohsaka, S. *et al.* STAT3 inhibition overcomes temozolomide resistance in glioblastoma by downregulating MGMT expression. *Mol. Cancer Ther.* **11**(6), 1289–1299 (2012).
33. Stechishin, O. D. *et al.* On-target JAK2/STAT3 inhibition slows disease progression in orthotopic xenografts of human glioblastoma brain tumor stem cells. *Neuro-oncology* **15**(2), 198–207 (2013).
34. Ma, J. *et al.* Reversing drug resistance of soft tumor-repopulating cells by tumor cell-derived chemotherapeutic microparticles. *Cell Res.* **26**(6), 713–727 (2016).
35. Chen, K. *et al.* The metabolic flexibility of quiescent CSC: Implications for chemotherapy resistance. *Cell Death Dis.* **12**(9), 835 (2021).
36. Huang, S., Chen, Y., Wu, J. & Chi, Y. Development and validation of novel risk prediction models of breast cancer based on stanniocalcin-1 level. *Cancer medicine.* **12**(6), 6499–6510 (2022).
37. Sengun, S. *et al.* Diagnostic and prognostic value of stanniocalcin 1 expression in papillary thyroid cancer. *Endocrine* **78**(1), 95–103 (2022).
38. Luo, W., Chen, D., Wang, H. & Hu, J. Stanniocalcin 1 is a prognostic biomarker in glioma. *Oncol. Lett.* **20**(3), 2248–2256 (2020).
39. Zhao, F. *et al.* HIF-1α-regulated stanniocalcin-1 mediates gemcitabine resistance in pancreatic ductal adenocarcinoma via PI3K/AKT signaling pathway. *Mol. Carcinog.* **61**(9), 839–850 (2022).
40. Lin, H. *et al.* Stanniocalcin 1 is a phagocytosis checkpoint driving tumor immune resistance. *Cancer Cell* **39**(4), 480-493.e486 (2021).
41. Peng, F. *et al.* Oncogenic AURKA-enhanced N(6)-methyladenosine modification increases DROSHA mRNA stability to transactivate STC1 in breast cancer stem-like cells. *Cell Res.* **31**(3), 345–361 (2021).
42. Li, Y. *et al.* Stanniocalcin-1 augments stem-like traits of glioblastoma cells through binding and activating NOTCH1. *Cancer Lett.* **416**, 66–74 (2018).
43. Lin, F. *et al.* Stanniocalcin 1 promotes metastasis, lipid metabolism and cisplatin chemoresistance via the FOXC2/ITGB6 signaling axis in ovarian cancer. *J. Exp. Clin. Cancer Res. CR* **41**(1), 129 (2022).
44. Chang, A. C. *et al.* STC1 expression is associated with tumor growth and metastasis in breast cancer. *Clin. Exp. Metastas.* **32**(1), 15–27 (2015).
45. Qing, Z. *et al.* MiR-144-3p targets STC1 to activate PI3K/AKT pathway to induce cell apoptosis and cell cycle arrest in selenium deficiency broilers. *J. Inorg. Biochem.* **226**, 111665 (2022).
46. Lu, L. *et al.* Cryptotanshinone inhibits human glioma cell proliferation by suppressing STAT3 signaling. *Mol. Cell Biochem.* **381**(1–2), 273–282 (2013).
47. Zhu, S. *et al.* Synergistic effect of cryptotanshinone and temozolomide treatment against human glioblastoma cells. *Sci. Rep.* **13**(1), 21835 (2023).
48. El-Tanani, M. *et al.* Importance of STAT3 signalling in cancer, metastasis and therapeutic interventions. *Cell. Signal.* **92**, 110275 (2022).
49. Khatoon, E. *et al.* The multifaceted role of STAT3 pathway and its implication as a potential therapeutic target in oral cancer. *Arch. Pharm. Res.* **45**(8), 507–534 (2022).
50. Tan, M. S. Y. *et al.* A STAT3-based gene signature stratifies glioma patients for targeted therapy. *Nat. Commun.* **10**(1), 3601 (2019).
51. Liu, Y. *et al.* STAT3/p53 pathway activation disrupts IFN-β-induced dormancy in tumor-repopulating cells. *J. Clin. Investig.* **128**(3), 1057–1073 (2018).
52. Liang, H., Chen, Z. & Sun, L. Inhibition of cyclin E1 overcomes temozolomide resistance in glioblastoma by Mcl-1 degradation. *Mol. Carcinog.* **58**(8), 1502–1511 (2019).
53. Wang, S. *et al.* Novel brain-stiffness-mimicking matrix gel enables comprehensive invasion analysis of 3D cultured GBM cells. *Front. Mol. Biosci.* **9**, 885806 (2022).
54. Chen, J. *et al.* Inhibition of cancer stem cell like cells by a synthetic retinoid. *Nat. Commun.* **9**(1), 1406 (2018).
55. Kanehisa, M. Toward understanding the origin and evolution of cellular organisms. *Protein Sci.* **28**(11), 1947–1951 (2019).

Acknowledgements

This work was supported by Key project of research and development of Hubei Province (Grant No. 2022BCE049); Natural Science Foundation of Hubei Province (Grant No. 2017CFA064); Fundamental Research Funds for the Central Universities (Grant No. 2015RC011); Taihe Hospital Foundation Project (grant no. 2022JJXM011). We would like to thank the Institute of Infection and Immunity for assistance in flow cytometry and Institute of Biological Medicine for assistance in luminescence detection.

Author contributions

C.D.: conceptualization, investigation, visualization, validation, writing—original draft, funding acquisition; B.H.: conceptualization, investigation; Y.W.: investigation, visualization; W.L.: writing—review & editing; W.B.: writing—review & editing; L.Y.: investigation; J.X.: investigation; H.G.: investigation; J.L.: writing—review & editing; Z.Y.: investigation; J.L.: investigation; W.T.: writing—review & editing; J.Q.: writing—review & editing, supervision; J.L.: writing—review & editing, supervision; Z.D.: conceptualization, data curation, writing—review & editing, project administration, supervision, funding acquisition. All authors have read and agreed to the published version of the manuscript.

Competing interests

The authors declare no competing interests.

Additional information

Supplementary Information The online version contains supplementary material available at https://doi.org/10.1038/s41598-024-68902-w.

Correspondence and requests for materials should be addressed to J.Q., J.L. or Z.D.